Anticancer Nanofibers

DOI: 10.1002/anie.201302658

Disruption of the Dynamics of Microtubules and Selective Inhibition of Glioblastoma Cells by Nanofibers of Small Hydrophobic Molecules**

*Yi Kuang and Bing Xu**

The self-organization of molecules through noncovalent interactions is able to generate complex matter and structures[1] that function at both supramolecular and cellular levels. For example, proteins self-assemble into a variety of nanofibers (or filaments), which are critical components of many essential cellular processes. Inside cells, actins, lamins, and tubulins undergo self-assembly to afford microfilaments, intermediate filaments, and microtubules, respectively;[2] outside cells, the self-assembly of collagen and elastin provides nanofibers that serve as an extracellular matrix to support and regulate the differentiation, proliferation, and interaction of cells.[2] The nanofibers of normal proteins are essential for normal cellular functions; however, the aggregation of aberrant proteins also results in aggregates (e.g., β-amyloid oligomers),[3] which are toxic to cells. Like proteins, certain small organic molecules also self-assemble in water to afford supramolecular nanofibers. In these processes, aromatic–aromatic interactions and hydrophobicity play critical roles in guiding hydrogen bonding, promoting self-assembly, and stabilizing the resulting nanofibers.[4] Although the successful formation of supramolecular nanofibers of small molecules has resulted in hydrogels[5] as a new class of biomaterials for tissue engineering,[6] drug delivery,[7] protein arrays,[8] electrophoresis,[9] bacteria typing,[10] and protocells,[11] there has been little exploration of the protein targets[12] and cytotoxicity of the supramolecular nanofibers of small molecules,[10,13] especially at concentrations below the critical gelation concentration (CGC).

Recently, Wells and co-workers reported that nanofibrils formed by the aggregation of small molecules would bind to procaspase-3 and activate its transformation into caspase-3 to initiate the apoptosis cascade.[13] Encouraged by this study and our previous results on cell death induced by the intracellular formation of molecular nanofibers,[14] we chose to evaluate the cytotoxicity of the versatile self-assembly motif **1** (Nap-FF; Figure 1a), which contains a naphthyl group and two phenylalanine residues. We selected **1** for three reasons: 1) **1** exhibits a remarkable ability to self-assemble in water and to form nanofibers at low concentration; 2) **1** has a known crystal structure,[15] which enabled us to infer a plausible molecular arrangement in the nanofibers formed by **1** (Figure 1b); 3) a close structural analogue of **1** exhibited specific interactions with certain protein targets (e.g., tubulins).[12] After determining the threshold concentration of **1** for the formation of molecular nanofibers, we incubated

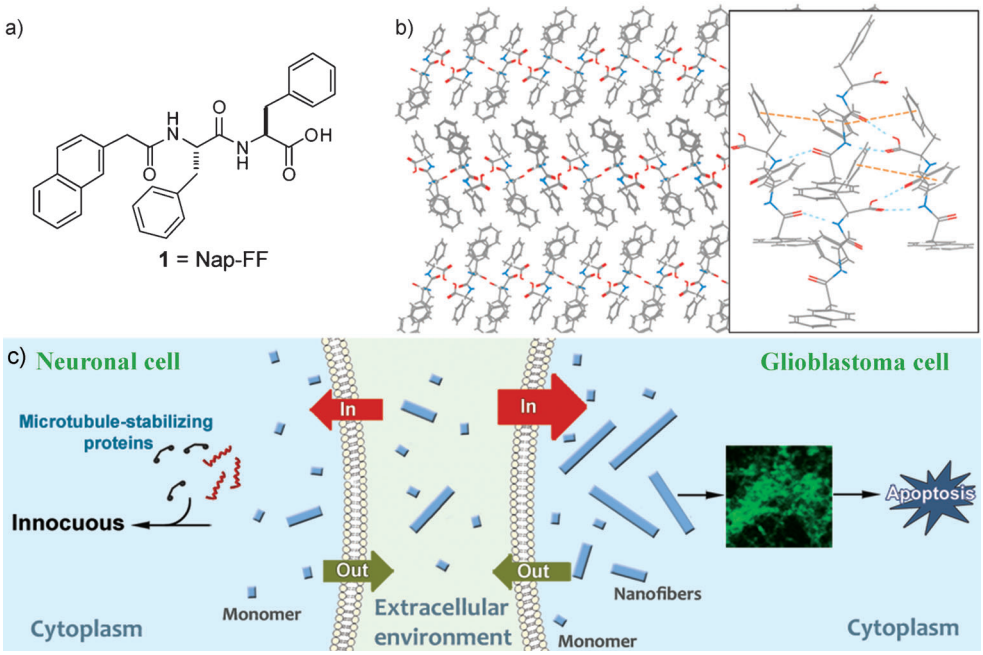

Figure 1. a) Chemical structure of **1**. b) Possible molecular arrangement (based on the crystal structure of **1**) in the nanofibers of **1**. The enlarged view shows hydrogen-bonding (cyan dashed lines) and aromatic–aromatic interactions (orange dashed lines) between the molecules. c) Proposed mechanism for the selective inhibition of the growth of glioblastoma cells by the supramolecular nanofibers of **1**.

[*] Y. Kuang, Prof. B. Xu
Department of Chemistry, Brandeis University
415 South Street, Waltham, MA 02453 (USA)
E-mail: bxu@brandeis.edu
Homepage: http://people.brandeis.edu/~bxu/

[**] This research was partially supported by the NIH (R01CA142746) and startup funds from Brandeis University. We acknowledge the help of the EM facility at Brandeis University. B.X. thanks Prof. N. Grigorieff for advice on TEM.

Supporting information for this article is available on the WWW under http://dx.doi.org/10.1002/anie.201302658.

cells with **1** at different concentrations and used a cell-based tubulin assay to elucidate the possible molecular targets of the nanofibers of **1**. Our results suggest that **1** self-assembles at and above 320–340 μM to form soluble nanofibers that disrupt the dynamics of microtubules and thus cause apoptosis of glioblastoma cells (Figure 1c). Notably, the nanofibers of **1** exhibited little acute toxicity towards a neuronal cell line (PC12). As the first example of the disruption of the self-organization of functional proteins by supramolecular nanofibers formed by the self-assembly of small molecules, this study not only indicates the potential therapeutic application of supramolecular nanofibers as anticancer agents to treat glioblastoma, a devastating disease without an effective cure, but also provides a mechanism for the inherent cytotoxicity of hydrophobic supramolecular nanofibers.

We first characterized the morphology of nanofibers formed by **1** and verified the threshold concentration of **1** for self-assembly. Molecules of **1** self-assemble efficiently to form nanofibers, which become entangled and hold water to form a hydrogel as a result of physical cross-linking (see Figure S1 in the Supporting Information). We found that **1** is able to self-assemble in water to form nanofibers below the CGC of **1** (0.4 wt%, 0.83 mM). We used transmission electron microscopy (TEM) to analyze solutions of **1** at different concentrations below the CGC of **1** in PBS buffer (phosphate-buffered saline; pH 7.4). Negatively stained[16] TEM images of **1** at 400 μM show nanofibers with a uniform width of 24 ± 2 nm as the dominant morphology (Figure 2a). We measured the length of all nanofibers in the TEM images and found a relatively wide distribution with an average value of about 181 nm (Figure 2b). In contrast, a TEM image of a solution of **1** at 300 μM only displayed amorphous features (see Figure S2), which suggests that **1** exists primarily in the monomeric state at a concentration of 300 μM and has a threshold concentration for the formation of nanofibers between 300 and 400 μM. The crystal structure of **1** suggests that aromatic–aromatic interactions and hydrogen bonding drive the self-assembly of **1** into β-strand-like structures (Figure 1b). Indeed, the circular dichroism (CD) spectrum of **1** at 400 μM correlates to a typical β-sheet structure according to the CD simulation of a negative peak at 190 nm followed by a positive peak at 200 nm (Figure 2c).[17] These results confirmed that nanofibers of **1** formed by the self-assembly of **1** adopt a β-sheet-like structure and led us to use thioflavin T (ThT), a benzothiazole dye that exhibits enhanced fluorescence upon binding to β-sheet-containing fibrils,[18] to quantify the self-assembly of **1**. At concentrations of **1** below 320 μM, the ThT emission showed little change; at and above a 340 μM concentration of **1**, the ThT emission increased linearly with the increase in the concentration of **1** (Figure 2d). These results indicate that the threshold concentration of **1** for the formation of nanofibers lies in the range of 320–340 μM.

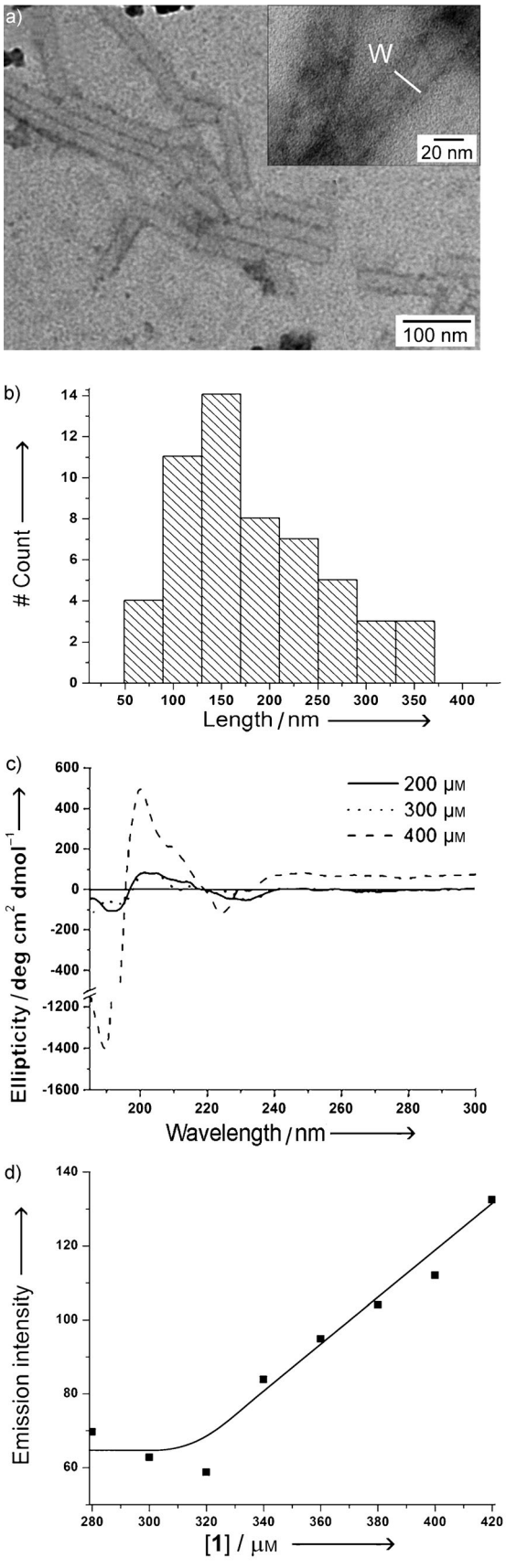

Figure 2. Characterization of molecular nanofibers of **1** in PBS buffer. a) Negatively stained TEM images of a solution of **1** (400 μM) in PBS buffer. b) Length distribution of the nanofibers as determined from TEM images of **1** (400 μM). c) Circular dichroism spectra of **1** at different concentrations. d) Emission of ThT (20 μM) at 484 nm ($\lambda_{ex} = 440$ nm) in the presence of **1** at increasing concentrations.

Furthermore, the fluorescence spectra of the solution of **1** at a concentration of 200 or 300 μM before and after filtration were essentially identical (see Figure S3), which are similar to the spectrum of monomeric naphthalene in water.[19] We therefore concluded that **1** mainly exists as a monomer at these concentrations.

We then examined the cytotoxicity of monomeric **1** and nanofibers of **1** by the incubation of mammalian cells with **1** at concentrations below and above the threshold for nanofiber formation. We first tested the cytotoxicity of **1** towards HeLa cells:[20] the most widely studied malignant cancer cell line.[21] Whereas monomers of **1** (i.e., **1** at 200 and 300 μM) exhibited little cytotoxicity, the presence of **1** at a concentration of 400 or 500 μM significantly decreased the viability of the HeLa cells to less than 20% within 48 h (Figure 3a). Above its threshold concentration for self-assembly, **1** exists as a mixture of nanofibers and monomers in solution. To verify that the nanofibers of **1** result in the cytotoxicity, we slowly passed the culture medium containing **1** through a nylon membrane with a pore size of 0.22 μm. Because of their size (Figure 2b), some of the nanofibers of **1** were removed by this filtration, but the monomers of **1** remained in the filtrate. Filtrates of the culture media containing **1** at a concentration of 400 or 500 μM exhibited less cytotoxicity towards HeLa cells (over 50% of the cells were viable after 48 h) than the corresponding unfiltered culture media (Figure 3b). This result agrees with that the concentrations of **1** in the solutions after filtration are below the threshold concentration for aggregation (see Table S1 in the Supporting Information). The above results suggest that the monomers of **1** are innocuous to cells, whereas the nanofibers of **1** inhibit the growth of HeLa cells.

To test whether the nanofibers of **1** inhibited the growth of other cancer cell lines in vitro, we incubated **1** with T98G cells,[22] a cancer cell line derived from glioblastoma, the most aggressive malignant primary brain tumor in humans.[23] The nanofibers of **1** also efficiently inhibited the growth of T98G cells, whereas monomers of **1** showed little cytotoxicity towards T98G (Figure 3c). In the brain, glial cells (from which glioblastoma originates) and neuronal cells together produce functional nervous systems.[24] We tested the cytotoxicity of **1** on the neuronal cell line PC12,[25] a frequently used model of neuronal cells.[26] Although nanofibers of **1** were acutely cytotoxic to T98G, both monomers and nanofibers of **1** exhibited little toxicity towards PC12 (Figure 3d). When the incubation of PC12 with nanofibers of **1** was prolonged for 7 days, over 60% of the PC12 cells still remained viable (see Figure S4). This result suggests that PC12 cells, unlike T98G, tolerate nanofibers of **1** to a certain degree.

An insidious facet of malignant cancer cells is that, unlike benign tumor cells, they ignore tissue boundaries and infiltrate or migrate into surrounding or distant tissues.[27] We therefore tested the influence of nanofibers of **1** on the

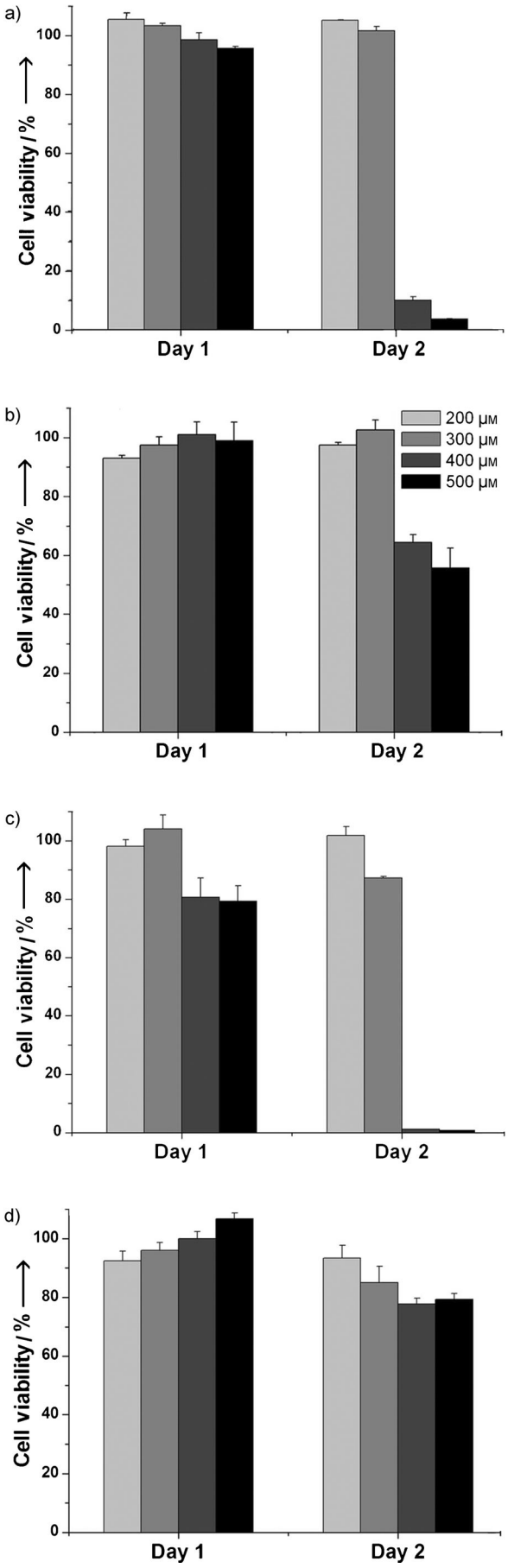

Figure 3. a,b) Cell-viability assays (3-(4,5-dimethylthiazol-2-yl)-2,5-diphenyltetrazolium bromide, MTT) of HeLa cells after treatment for 24 and 48 h with as-prepared (a) or filtered medium (b) containing **1** at different initial concentrations. c,d) MTT assays of T98G (c) and PC12 cell lines (d) incubated with **1**.

migration of HeLa cells. We first created a gap with a width of 0.9 mm by placing a plastic insert on a fully confluent layer of HeLa cells (Figure 4a) and then applied media containing **1** at different concentrations. During a culture period of 18 h, the untreated cells and the cells incubated with **1** at a concentration of 300 μM exhibited similar rates of migration and covered 47% of the gap (Figure 4b,c). When incubated with

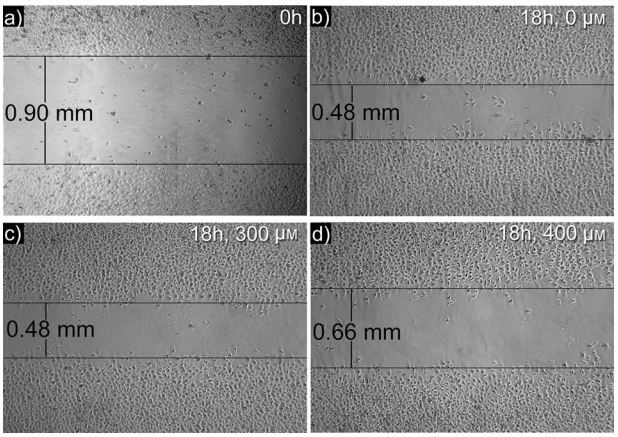

Figure 4. Cell-migration assay of HeLa cells treated with **1**. a) A gap was created on a layer of HeLa cells of 100% confluence in 24-well plates, and the size of the gap was measured after incubation for 18 h with **1** at a concentration of b) 0, c) 300, or d) 400 μM.

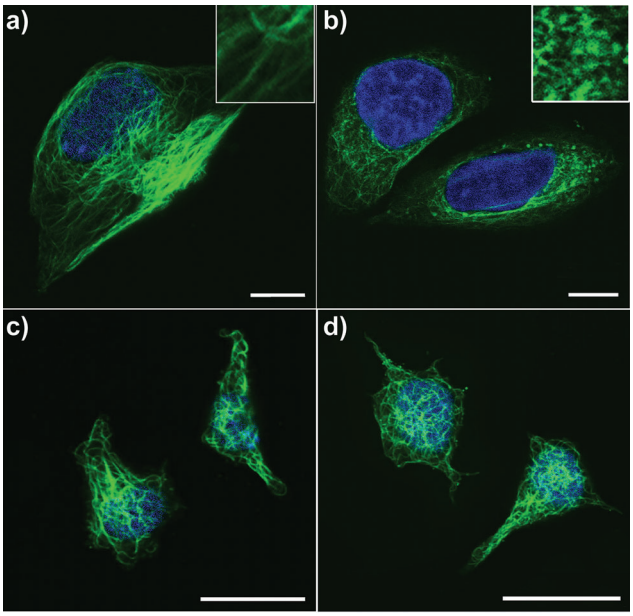

Figure 5. Confocal images of tubulin-stained a,b) T98G and c,d) PC12 cells treated with medium containing **1** at a concentration of 0 (a,c) or 400 μM (b,d) for 24 h. DNA was counterstained blue with 4′-6-diamidino-2-phenylindole (DAPI). Insets are images that have been enlarged further by a factor of 3. Scale bar: 10 μm.

1 at a concentration of 400 μM, the cells only covered 27% of the gap (Figure 4d). These results indicate that nanofibers of **1** delay the migration of cells. Since microtubules and filamentous actin are essential for establishing and maintaining cell migration,[28] we speculate that nanofibers of **1** may affect the function of either microtubules or filamentous actin to delay cell migration. This result agrees with an in vitro experiment in our previous study, which showed that the nanofibers of a photoreactive hydrogelator that is structurally similar to **1** selectively bind tubulin.[12]

To verify the speculation that the nanofibers of **1** could interact with tubulin, we used tubulin tracker to visualize microtubules in T98G and PC12 cells incubated with or without nanofibers of **1** for 24 h. The untreated T98G cells displayed a long microtubule network that stretched through the cell body (Figure 5a). When T98G cells were treated with **1** at a concentration of 400 μM (i.e., with nanofibers of **1**), tubulins in the T98G cells aggregated into clusters with scattered microtubule filaments (Figure 5b). This result indicates that the nanofibers of **1** disrupt the dynamics of microtubules. The time-dependent cytotoxicity curve of nanofibers of **1** shows that cancer cells enter the death phase after incubation for 38 h (see Figure S5); thus, the disruption of microtubules occurs prior to cell death. As it is known that malfunction of microtubules can lead to apoptosis,[29] we used apoptosis assays (fluorescein isothiocyanate–annexin V, propidium iodide, and terminal deoxynucleotidyl transferase dUTP nick end labeling (TUNEL))[30] to evaluate T98G cells treated with **1** (400 μM) for 24 h. The results of the assays confirm that the T98G cells enter the early stage of apoptosis (see Figure S6). These data together suggest that the nanofibers of **1** disrupt the dynamics of microtubules and consequently induce apoptosis of glioblastoma cells (e.g., T98G). Moreover, the HeLa cells enter the death phase after 38 h regardless of the concentration (400 or 500 μM) of **1**, in agreement with the hypothesis that the aggregates of **1** cause cell death and that the cytotoxicity of **1** deviates from the conventional dosage response based on the concentration of the monomers. Unlike in T98G cells, microtubules in PC12 cells treated with nanofibers of **1** exhibited little change in comparison with those in untreated PC12 cells (Figure 5c,d); thus, microtubules in PC12 cells appear to tolerate treatment with **1**. The reasons for the significant microtubule disruption in T98G cells and the consequently higher cytotoxicity of **1** than that observed for PC12 cells lie in the accelerated metabolic rate of glioblastoma cells as a result of the Warburg effect[31] and the tendency of small molecules to accumulate in cells once they have formed aggregates.[14b] Since **1** accumulates much more slowly in PC12 cells than in T98G cells (see Figure S7), the amount of nanofibers of **1** in PC12 cells is much less than that in T98G cells. Thus, **1** induces little microtubule disruption and little cytotoxicity in PC12 cells.

In conclusion, this study establishes that supramolecular nanofiber assemblies of small molecules exhibit properties drastically different from those of the individual molecules when they interact with cells. Moreover, the hydrophobicity of **1** appears to be critical to the observed cytotoxicity, because an analogue **2**, obtained by replacement of the phenylalanine residues (F) in **1** with tyrosine residues (Y), exhibited a relatively high critical aggregation concentration (1.0 mM) and considerably lower cytotoxicity (see Figure S8).

Considering the relatively high hydrophobicity of **1**, which has higher logP value (4.57) than that of naphthalene ($\log P = 3.03$), the results of the cell-based tubulin assay imply that the inherent toxicity of other nanofibers with a high local density of hydrophobicity might also arise from a similar mechanism. A cell-based assay is necessary for the elucidation of the molecular mechanism of such nanofibers, as shown by the elucidation of the molecular mechanism of nanofibers of **1**. Moreover, the successful inhibition of the growth of glioblastoma cells without detrimental effects to neuronal cells highlights the potential of the therapeutic application of supramolecular nanofibers or aggregates of small hydrophobic molecules, as a type of "de novo molecular amyloids", in the treatment of this most aggressive malignant brain tumor. In ongoing studies, we are engineering the temporal profiles of the supramolecular nanofibers to enable the desired therapeutic effect.

Experimental Section

Materials and methods: All chemicals and reagents were obtained from FisherSci. Circular dichroism was performed with a JASCO J-810 spectrometer, transmission electron microscopy with a Morgagni 268 transmission electron microscope, the MTT (3-(4,5-dimethylthiazol-2-yl)-2,5-diphenyltetrazolium bromide) viability assay and tubulin-polymerization assay with a DTX 880 multimode detector, flow cytometry with a FACSCalibur flow cytometer, isothermal titration calorimetry with a NANO ITC Low Volume instrument (TA instruments), and fluorescence spectroscopy with an RF-5301PC spectrofluorophotometer; confocal images were taken with a Leica SP2 microscope.

Tubulin staining:[32] Cells in the exponential growth phase were seeded in a glass-bottomed culture chamber at 10000 cell mL^{-1} and left for 24 h at 37 °C (5% CO_2) to enable attachment. The culture medium was then removed, and new culture medium containing **1** (0 or 400 μM) was added. After incubation for 24 h, cells were washed with PBS buffer three times and stained with Tubulin Tracker Green (100 nM) and DAPI (300 nM) in PBS for 30 min at 37 °C in the dark. The sample was rinsed three times with PBS, and the cells were kept in PBS for imaging.

Received: March 30, 2013
Published online: May 17, 2013

Keywords: antitumor agents · cancer · nanostructures · self-assembly · tubulin

[1] a) J. M. Lehn, *Science* **2002**, *295*, 2400 – 2403; b) G. M. Whitesides, J. P. Mathias, C. T. Seto, *Science* **1991**, *254*, 1312 – 1319; c) G. M. Whitesides, B. Grzybowski, *Science* **2002**, *295*, 2418 – 2421.

[2] H. Lodish, A. Berk, P. Matsudaira, C. A. Kaiser, M. Krieger, M. P. Scott, S. L. Zipursky, J. Darnell, *Mol. Cell Biol.*, Freeman, New York, **2003**.

[3] I. Cherny, E. Gazit, *Angew. Chem.* **2008**, *120*, 4128 – 4136; *Angew. Chem. Int. Ed.* **2008**, *47*, 4062 – 4069.

[4] a) A. Brizard, M. Stuart, K. van Bommel, A. Friggeri, M. de Jong, J. van Esch, *Angew. Chem.* **2008**, *120*, 2093 – 2096; *Angew. Chem. Int. Ed.* **2008**, *47*, 2063 – 2066; b) M. L. Ma, Y. Kuang, Y. Gao, Y. Zhang, P. Gao, B. Xu, *J. Am. Chem. Soc.* **2010**, *132*, 2719 – 2728; c) P. Martín-Gago, M. Gomez-Caminals, R. Ramón, X. Verdaguer, P. Martin-Malpartida, E. Aragón, J. Fernández-Carneado, B. Ponsati, P. López-Ruiz, M. A. Cortes, B. Colás, M. J. Macias, A. Riera, *Angew. Chem.* **2012**, *124*, 1856 – 1861; *Angew. Chem. Int. Ed.* **2012**, *51*, 1820 – 1825.

[5] L. A. Estroff, A. D. Hamilton, *Chem. Rev.* **2004**, *104*, 1201 – 1217.

[6] A. M. Smith, R. J. Williams, C. Tang, P. Coppo, R. F. Collins, M. L. Turner, A. Saiani, R. V. Ulijn, *Adv. Mater.* **2008**, *20*, 37 – 41.

[7] a) F. Zhao, M. L. Ma, B. Xu, *Chem. Soc. Rev.* **2009**, *38*, 883 – 891; b) J. C. Tiller, *Angew. Chem.* **2003**, *115*, 3180 – 3183; *Angew. Chem. Int. Ed.* **2003**, *42*, 3072 – 3075.

[8] S. Kiyonaka, K. Sada, I. Yoshimura, S. Shinkai, N. Kato, I. Hamachi, *Nat. Mater.* **2004**, *3*, 58 – 64.

[9] S. Yamamichi, Y. Jinno, N. Haraya, T. Oyoshi, H. Tomitori, K. Kashiwagi, M. Yamanaka, *Chem. Commun.* **2011**, *47*, 10344 – 10346.

[10] Z. M. Yang, P. L. Ho, G. L. Liang, K. H. Chow, Q. G. Wang, Y. Cao, Z. H. Guo, B. Xu, *J. Am. Chem. Soc.* **2007**, *129*, 266 – 267.

[11] R. Krishna Kumar, X. X. Yu, A. Patil, M. Li, S. Mann, *Angew. Chem.* **2011**, *123*, 9515 – 9519; *Angew. Chem. Int. Ed.* **2011**, *50*, 9343 – 9347.

[12] Y. Gao, M. J. C. Long, J. Shi, L. Hedstrom, B. Xu, *Chem. Commun.* **2012**, *48*, 8404 – 8406.

[13] J. A. Zorn, H. Wille, D. W. Wolan, J. A. Wells, *J. Am. Chem. Soc.* **2011**, *133*, 19630 – 19633.

[14] a) Z. M. Yang, K. M. Xu, Z. F. Guo, Z. H. Guo, B. Xu, *Adv. Mater.* **2007**, *19*, 3152 – 3156; b) Z. M. Yang, G. L. Liang, Z. F. Guo, Z. H. Guo, B. Xu, *Angew. Chem.* **2007**, *119*, 8364 – 8367; *Angew. Chem. Int. Ed.* **2007**, *46*, 8216 – 8219.

[15] Y. Zhang, Y. Kuang, Y. A. Gao, B. Xu, *Langmuir* **2011**, *27*, 529 – 537.

[16] L. L. Frado, R. Craig, *J. Mol. Biol.* **1992**, *223*, 391 – 397.

[17] N. J. Greenfield, *Nat. Protoc.* **2007**, *1*, 2876 – 2890.

[18] H. Levine, *Protein Sci.* **1993**, *2*, 404 – 410.

[19] S. Lee, M. A. Winnik, *Can. J. Chem.* **1993**, *71*, 1216 – 1224.

[20] K. A. Rafferty, *Virchows Arch. B* **1986**, *50*, 167 – 180.

[21] R. Skloot, *The Immortal Life of Henrietta Lacks*, Crown, New York, **2010**.

[22] A. Schlenska-Lange, H. Knüpfer, T. J. Lange, W. Kiess, M. Knüpfer, *Anticancer Res.* **2008**, *28*, 1055 – 1060.

[23] M. Rubenstein, M. Shaw, Z. Mirochnik, L. Slobodskoy, R. Glick, T. Lichtor, P. Chou, P. Guinan, *Methods Find. Exp. Clin. Pharmacol.* **1999**, *21*, 391 – 393.

[24] E. A. Maher, F. B. Furnari, R. M. Bachoo, D. H. Rowitch, D. M. Louis, W. K. Cavenee, R. A. DePinho, *Genes Dev.* **2001**, *15*, 1311 – 1333.

[25] Y. Cheng, I. Zhizhin, R. L. Perlman, D. Mangoura, *J. Biol. Chem.* **2000**, *275*, 23326 – 23332.

[26] C. M. Troy, M. L. Shelanski, *Proc. Natl. Acad. Sci. USA* **1994**, *91*, 6384 – 6387.

[27] A. Giese, R. Bjerkvig, M. E. Berens, M. Westphal, *J. Clin. Oncol.* **2003**, *21*, 1624 – 1636.

[28] O. C. Rodriguez, A. W. Schaefer, C. A. Mandato, P. Forscher, W. M. Bement, C. M. Waterman-Storer, *Nat. Cell Biol.* **2003**, *5*, 599 – 609.

[29] S. W. Sherwood, J. P. Sheridan, R. T. Schimke, *Exp. Cell Res.* **1994**, *215*, 373 – 379.

[30] G. Del Bino, Z. Darzynkiewicz, C. Degraef, R. Mosselmans, D. Fokan, P. Galand, *Cell Proliferation* **1999**, *32*, 25 – 37.

[31] P. P. Hsu, D. M. Sabatini, *Cell* **2008**, *134*, 703 – 707.

[32] D. J. Koss, K. P. Hindley, G. Riedel, B. Platt, *J. Neurochem.* **2007**, *102*, 1009 – 1023.

